Orthogonal Exponential Spline Pulses with Application to Impulse Radio

Masaru Kamada, Semih Özlem, Hiromasa Habuchi

Orthogonal Exponential Spline Pulses with Application to Impulse Radio

Masaru Kamada[(1)], Semih Özlem[(2)] and Hiromasa Habuchi[(1)]

(1) Ibaraki University, Hitachi, Ibaraki 316 8511, Japan.
(2) Bogazici University, Bebek, Istanbul, Turkey.
kamada@mx.ibaraki.ac.jp, semozl@gmail.com, habuchi@mx.ibaraki.ac.jp

Abstract:

With application to the impulse radio communications in mind, a locally supported and zero-mean pulse which is orthogonal to its shifts by integers is sought among the exponential splines having the knot interval $\frac{1}{2}$. An example pulse is obtained that complies with the regulation imposed by the US Federal Communications Commission and will potentially enable an impulse radio communications system as fast as 6G pulses per second.

1. Introduction

The M-shaped linear spline

$$M(t) = \begin{cases} \sqrt{3}t, & 0 \le t \le \frac{1}{2} \\ \sqrt{3}(2-3t), & \frac{1}{2} \le t \le 1 \\ \sqrt{3}(3t-4), & 1 \le t \le \frac{3}{2} \\ \sqrt{3}(2-t), & \frac{3}{2} \le t \le 2 \\ 0, & \text{elsewhere} \end{cases} \tag{1}$$

plotted in Fig. 1 is not a wavelet in the sense of muntiresolutional analysis because $M(t)$ is not orthogonal to its contracted version $M(2t)$. But it has three remarkable properties that (i) it is locally supported, (ii) its integration over the domain is zero, and (iii) its shifts by integers are orthogonal to one another [2]. Those properties are exactly what is required of pulses for the impulse radio communications [6]. The three properties are required (i) for the sake of real-time communications, (ii) for the pulse to be feasible as a radio waveform, and (iii) for pulse detection to be robust against noise in the sense of least-square estimation, respectively.

We shall look for this kind of pulse functions in the broader family of exponential splines [4, 5] which have the advantage that they can be shaped through linear dynamical systems [5] . The pulse functions, if they are found, will work as practical pulses which carry information in the impulse radio communications.

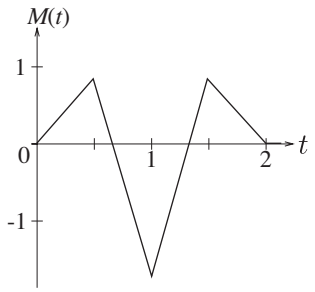

Figure 1: M-shaped linear spline.

The problem is simple: we are to find a locally supported and zero-mean exponential spline $q(t)$ with the knot interval $\frac{1}{2}$ that satisfies

$$\int_{-\infty}^{\infty} q(t)q(t-k)dt = \begin{cases} 1, & k=0 \\ 0, & k \neq 0 \end{cases} \tag{2}$$

for any ingeter k. This paper presents a procedure to find such a pulse function and its application to the impulse radio.

2. Construction of orthogonal pulses

Any exponential spline can be represented by a linear combination of the exponential B-spline and its shifts [4, 5]. An exponential B-spline with the knot interval $\frac{1}{2}$ is the output

$$\beta(t) = S(b)(t) \tag{3}$$

of a linear dynamical system S having the transfer function

$$G(s) = \frac{\mu_{n-1}s^{n-1} + \cdots + \mu_1 s + \mu_0}{(s-\lambda_0)(s-\lambda_1)\cdots(s-\lambda_{n-1})} \tag{4}$$

for the input being a series of delta functions

$$b(t) = \sum_{l=0}^{n} b_l \delta(t - l/2) \tag{5}$$

such that

$$\begin{aligned} B(z) &= \sum_{l=0}^{n} b_l z^{-\frac{l}{2}} \\ &= (1-z^{-\frac{1}{2}}\mathrm{e}^{\frac{\lambda_0}{2}})(1-z^{-\frac{1}{2}}\mathrm{e}^{\frac{\lambda_1}{2}})\cdots(1-z^{-\frac{1}{2}}\mathrm{e}^{\frac{\lambda_{n-1}}{2}}). \end{aligned} \tag{6}$$

This exponential B-spline is locally supported as

$$\beta(t) = 0, \ \ t \notin \left(0, \frac{n}{2}\right). \tag{7}$$

In order to keep the splines zero-mean, instead of the original exponential B-spline $\beta(t)$, we shall use

$$\alpha(t) = \beta(t) - \beta\left(t - \frac{1}{2}\right) \tag{8}$$

which has the zero mean

$$\int_{-\infty}^{\infty}\alpha(t)dt=0 \tag{9}$$

and is locally supported as

$$\alpha(t)=0,\ \ t\notin\left(0,\frac{n+1}{2}\right). \tag{10}$$

Another representation of this $\alpha(t)$ is the output

$$\alpha(t)=S(a)(t) \tag{11}$$

of S for the input

$$a(t)=\sum_{l=0}^{n}a_l\delta(t-l/2), \tag{12}$$

where

$$\begin{aligned}A(z)=&\sum_{l=0}^{n+1}a_lz^{-\frac{l}{2}}\\ =&(1-z^{-\frac{1}{2}}\mathrm{e}^{\frac{\lambda_0}{2}})\cdots(1-z^{-\frac{1}{2}}\mathrm{e}^{\frac{\lambda_{n-1}}{2}})(1-z^{-\frac{1}{2}}).\end{aligned} \tag{13}$$

Let the desired pulse function be represented in the form

$$q(t)=\sum_{l=0}^{n-1}c_l\alpha(t-l/2). \tag{14}$$

Then it is automatic that $q(t)$ is locally supported as

$$q(t)=0,\ \ t\notin(0,n) \tag{15}$$

and has the zero mean

$$\int_{-\infty}^{\infty}q(t)dt=0. \tag{16}$$

The remaining request is that its autocorrelation

$$r(x)=\int_{-\infty}^{\infty}q(t)q(t-x)dt \tag{17}$$

should satisfy the orthogonality conditions

$$r(k)=\begin{cases}1, & k=0\\ 0, & k=\pm1,\pm2,\cdots\end{cases} \tag{18}$$

with respect to shift by integers. Here the number n of $\{\alpha(t-l/2)\}_{l=0}^{n-1}$ employed for composing $q(t)$ in (14) is chosen so that the number n of the unknown coefficients $\{c_l\}_{l=0}^{n-1}$ be the same as that of the essential conditions

$$r(k)=\begin{cases}1, & k=0\\ 0, & k=1,2,\cdots,n-1\end{cases} \tag{19}$$

reduced from (18) by (15) and the equality $r(x)=r(-x)$.

Now we have only to find the coefficients $\{c_l\}_{l=0}^{n-1}$ that make (19) hold good. Define

$$c(t)=\sum_{l=0}^{n-1}c_l\delta(t-l/2)\ \ \text{and}\ \ C(z)=\sum_{l=0}^{n-1}c_lz^{-\frac{l}{2}} \tag{20}$$

by $\{c_l\}_{l=0}^{n-1}$, and prepare time-reversed functions

$$\tilde{a}(t)=a(-t),\ \tilde{c}(t)=c(-t),\ \tilde{q}(t)=q(-t) \tag{21}$$

and the "mirror" system $\tilde{S}$ having the transfer function $G(-s)$. Then we can express the correlation by

$$\begin{aligned}r(k)\ &=\ (q*\tilde{q})(k)\\ &=\ (S\circ\tilde{S})(a*\tilde{a}*c*\tilde{c})(k),\end{aligned} \tag{22}$$

where $*$ denotes the convolution integral, and we can write $D(z)=C(z)C(z^{-1})$ in the form

$$C(z)C(z^{-1})=d_0+\sum_{j=1}^{n-1}d_j(z^{-\frac{j}{2}}+z^{\frac{j}{2}}) \tag{23}$$

which implies

$$(c*\tilde{c})(t)=\ d_0\delta(t)+\sum_{j=1}^{n-1}d_j\left(\delta(t-j/2)+\delta(t+j/2)\right). \tag{24}$$

In the meantime, a locally supported exponential spline

$$\varphi(x)=(S\circ\tilde{S})(a*\tilde{a})(x) \tag{25}$$

associated with the composite system $S\circ\tilde{S}$ satisfies

$$\varphi(x)=\varphi(-x). \tag{26}$$

By (22), (24), (25) and (26), we can reduce the orthogonality conditions (19) to the linear equations

$$\begin{aligned}&d_0\varphi(k)+\sum_{j=1}^{n-1}d_j\left(\varphi(k-j/2)+\varphi(k+j/2)\right)\\ =&\begin{cases}1, & k=0\\ 0, & k=1,2,\cdots,n-1.\end{cases}\end{aligned} \tag{27}$$

Solvability of (27) for $\{d_j\}_{j=0}^{n-1}$ can be checked by numerical computation in practice. A simpler condition in terms of dynamical parameters is yet to be established.

We assume that (27) is solvable since we cannot proceed unless this is the case. Then, $C(z)C(z^{-1})$ determined by (23) from $\{d_j\}_{j=0}^{n-1}$ can be factorized in the form

$$\begin{aligned}C(z)C(z^{-1})=\gamma_0&(z^{-\frac{1}{2}}-\gamma_1)(z^{\frac{1}{2}}-\gamma_1)(z^{-\frac{1}{2}}-\gamma_2)(z^{\frac{1}{2}}-\gamma_2)\\ &\cdots(z^{-\frac{1}{2}}-\gamma_{n-1})(z^{\frac{1}{2}}-\gamma_{n-1}).\end{aligned} \tag{28}$$

Taking half the factors, we can find

$$C(z)=\pm\sqrt{\gamma_0}(z^{-\frac{1}{2}}-\gamma_1)(z^{-\frac{1}{2}}-\gamma_2)\cdots(z^{-\frac{1}{2}}-\gamma_{n-1}) \tag{29}$$

that gives the sought coefficients $\{c_l\}_{l=0}^{n-1}$ by (20). Exciting the system S with the input series of delta functions

$$v(t)=\sum_{l=0}^{n-1}c_la(t-l/2), \tag{30}$$

we obtain the desired pulse function

$$q(t)=S(v)(t)=\sum_{l=0}^{n-1}c_l\alpha(t-l/2). \tag{31}$$

In the case $G(s) = \frac{1}{s}$, the problem is trivial and the resulting pulse is the Haar function

$$H(t) = \begin{cases} 1, & 0 < t \le \frac{1}{2} \\ -1, & \frac{1}{2} < t \le < 1 \\ 0, & \text{elsewhere.} \end{cases} \quad (32)$$

The case $G(s) = \frac{1}{s^2}$ yields $M(t)$ of (1) as expected. Because it happens that $M(t) = \sqrt{3}(H * H)(t)$, we might speculate that the pulse associated with $G(s) = \frac{1}{s^3}$ could be proportional to $(H*H*H)(t)$. But that is not true since $(H * H * H)(t)$ is not orthogonal to $(H * H * H)(t-2)$. It is interesting as well as disappointing that we obtain a complex-valued pulse in the case $G(s) = \frac{1}{s^3}$. A nice example pulse will appear in the next section in the context of its application to the impulse radio communications.

3. Application to Impulse Radio

While the series of delta functions $a(t)$ does not exist in the real world, its integration

$$\int_{-\infty}^{t} a(\tau)d\tau = \begin{cases} 0, \ t < 0 \\ \sum_{k=0}^{l} a_k, \ \frac{l}{2} < t < \frac{l+1}{2}, l = 0, 1, \cdots, n \\ \sum_{k=0}^{n+1} a_k = A(1) = 0, \ \frac{n+1}{2} < t \end{cases} \quad (33)$$

is a locally supported piecewise constant function that can be easily generated by electric current switches.

The system S excited by the piecewise constant function

$$u(t) = \int_{-\infty}^{t} v(\tau)d\tau = \sum_{l=0}^{n} c_l \int_{-\infty}^{t-l/2} a(\tau)d\tau \quad (34)$$

shapes the pulse

$$p(t) = S(u)(t) \quad (35)$$

which is locally supported as

$$p(t) = 0, \quad t \notin (0, n) \quad (36)$$

and has the relationship

$$p(t) = \sum_{l=0}^{n} c_l \int_{-\infty}^{t-l/2} \alpha(\tau)d\tau = \int_{-\infty}^{t} q(\tau)d\tau. \quad (37)$$

Besides the simple and practical system (35) to shape $p(t)$ from the piecewise constant seed $u(t)$, the pulse $p(t)$ has the remarkable property

$$\int_{-\infty}^{\infty} \frac{d^2}{dt^2}p(t)\ p(t-k)dt = -\int_{-\infty}^{\infty} q(t)q(t-k)dt = \begin{cases} -1, & k = 0 \\ 0, & k = \pm 1, \pm 2, \cdots \end{cases} \quad (38)$$

which follows from (17), (18), (36), (37) and the partial integration formula. This property gives the foundation to transmission and detection of the pulse $p(t)$ in the impulse radio communications.

Given data bits $\{w_l\}$, we transmit the waveform

$$w(t) = S\left(\sum_{l=-\infty}^{\infty} w_l u(t-l)\right) = \sum_{l=-\infty}^{\infty} w_l p(t-l) \quad (39)$$

as illustrated in Fig. 2. Since a good broadband antenna is well approximated [6] by $\frac{d}{dt}$, the transmitted signal $w(t)$ is differentiated once by the transmitter antenna to be the radio signal

$$\frac{d}{dt}w(t) = \sum_{l=-\infty}^{\infty} w_l \frac{d}{dt}p(t-l) \quad (40)$$

and again by the receiver antenna to arrive at the receiver as

$$\frac{d^2}{dt^2}w(t) = \sum_{l=-\infty}^{\infty} w_l \frac{d^2}{dt^2}p(t-l). \quad (41)$$

Correlating the received signal $\frac{d^2}{dt^2}w(t)$ with the template pulse $p(t-k)$, which is the same as the transmission pulse, for its duration $(k, k+n)$, we have the bit w_k recovered by

$$\begin{aligned} \int_k^{k+n} \frac{d^2}{dt^2}w(t)\ p(t-k)dt &= \int_{-\infty}^{\infty} \frac{d^2}{dt^2}w(t)\ p(t-k)dt \\ &= \sum_{l=-\infty}^{\infty} w_l \int_{-\infty}^{\infty} \frac{d^2}{dt^2}p(t-l)\ p(t-k)dt \\ &= -w_k \end{aligned} \quad (42)$$

because of the property (38).

It should be noted that, because of (38), the detection formula (42) virtually performs the least-squares approximation of the radio waveform $\frac{d}{dt}w(t)$ by $\frac{d}{dt}p(t-k) = q(t-k)$ to detect w_k. Additive noises superimposed on $\frac{d}{dt}w(t)$ will then be most suppressed in the sense of least-squares estimation.

An example pulse associated with the transfer function

$$G(s) = \frac{1}{(s+18)(s+11.1i+10^{-13})(s-11.1i+10^{-13})} \quad (43)$$

and its derivatives are plotted in Fig. 3. The correlation in Fig. 4 becomes 1 and 0 at the origin and at the other integers, respectively, to verify (38). The power spectral density of the radio pulse $\frac{d}{dt}p(t) = q(t)$ is plotted in Fig. 5 along with the spectral mask (plotted by the boxy line) for the indoor ultra-wideband communications systems [1] imposed by the US Federal Communications Commission

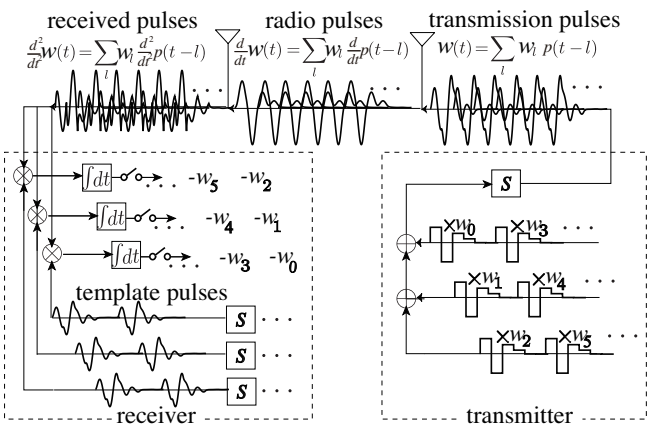

Figure 2: Schematic diagram of the transceiver.

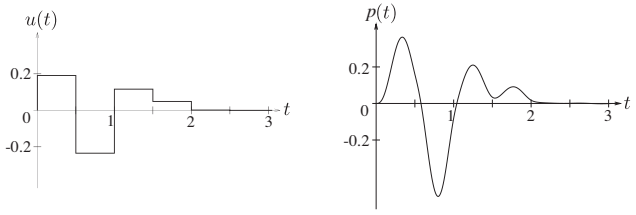

(a) pulse seed $u(t)$

(b) transmission pulse $p(t)$

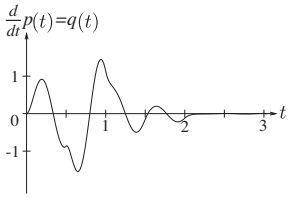

(c) radio pulse $\frac{d}{dt}p(t)$

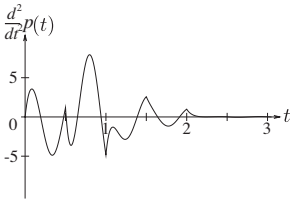

(d) received pulse $\frac{d^2}{dt^2}p(t)$

Figure 3: Pulses for impulse radio.

as the upper bound which no practical pulses are allowed to exceed. The frequency axis of the mask is scaled down by 6 GHz for the purpose of comparison, or equivalently, the pulse repetition rate is assumed to be 6 G pulses per second, which is much faster than the 1.32G pulses per second of the high speed direct sequence ultra-wideband protocol discussed in the IEEE 802.15.3a standard.

The fast transmission is possible because the pulses are orthogonal even though they are densely overlapping. But dense pulses are prone to interfere with one another in the situation that several reflected pulses arrive with various delays. Multipath compensation by digital filtering is crucial in order to effectively exploit the dense pulses we obtained. Transmitting a sounder pulse and digitizing the observed correlations, we have the end-to-end impulse response of the multipath channel. Digital filtering by an FIR approximation of the inverse impulse response will work as a kind of rake receiver. This compensation requires an analog-to-digital converter and a digital filter that work at the pulse rate and thus costs more hardware. But this cost should be justified since all the pulse-based systems cannot be faster without having denser pulses in the first place. A detailed analysis of the multipath effects, channel modeling error, and pulse synchronization is available in [3].

We may ignore the multipath effects and channel modeling error in the extreme situation that antennas are inductively coupled at a very short distance less than one inch. TransferJet technology has been working in the same situation at the maximum transmission rate of 560Mbps since 2008. A faster system will hopefully be the first application of the dense pulses obtained in this paper.

4. Conclusions

Inspired by the M-shaped orthogonal pulse, we derived a procedure to construct an exponential spline pulse with the knot interval $\frac{1}{2}$ that is locally supported, has its mean zero, and is orthogonal to its shifts by integers. An example pulse was obtained that will potentially enable an impulse radio communications system as fast as 6G pulses per second under the FCC regulation for the indoor ultra-wideband communications.

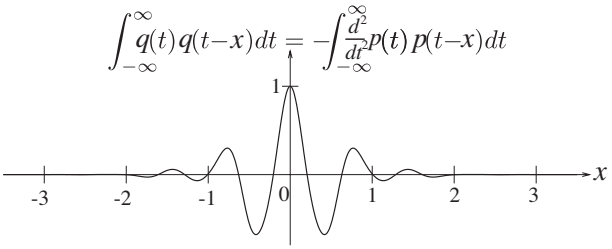

Figure 4: Correlation of the pulse.

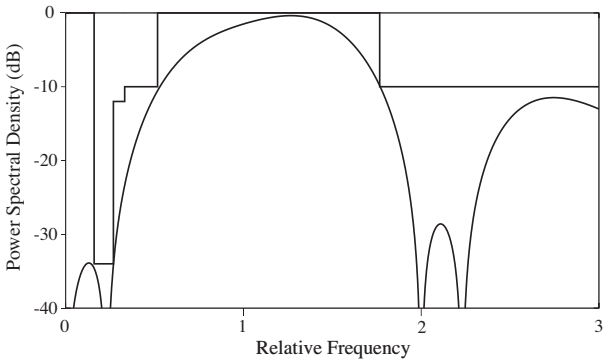

Figure 5: Power spectral density of the pulse and the FCC spectral mask.

5. Acknowledgment

This work was partially supported by JSPS grant-in-aid No. 17560357.

References:

[1] *Revision of Part 15 the Commission's rule regarding ultra-wideband transmission systems*. ET Docket No.98-153, Federal Communications Commission, Washington, D.C., 2002.

[2] A. J. Jerri. *Wavelets – Detailed Treatment with Applications*. Exercises of Chapter 3. Sampling Publishing, Potsdam, NY, to appear in 2009.

[3] M. Kamada S. Özlem and H.Habuchi. Construction of orthogonal overlapping pulses for impulse radio communications. *IEICE Transactions on Fundamentals*, E91-A(11):3121–3129, Nov. 2008.

[4] M. Unser and T. Blu. Cardinal exponential splines: Part I—Theory and filtering algorithms. *IEEE Transactions on Signal Processing*, 53(4):1425–1438, April 2005.

[5] M. Unser. Cardinal exponential splines: Part II—Think analog, act digital. *IEEE Transactions on Signal Processing*, 53(4):1439–1449, April 2005.

[6] M. Z. Win and R. A. Scholtz. Impulse radio: how it works. *IEEE Commun. Lett.*, 2(2):36–38, 1988.